WINGLET AND LONG-DUCT NACELLE AERODYNAMIC DEVELOPMENT FOR DC-10 DERIVATIVES*

by

A. Brian Taylor
Douglas Aircraft Company
Long Beach, California

SUMMARY

Two promising advances are under development for application to near-term derivatives of the Douglas DC-10 transport. The winglet, a near-vertical surface at the wing tip, offers substantial cruise drag reduction with less wing root bending moment penalty than a wing-tip extension of the same effectiveness. Wind tunnel tests have confirmed these predictions. The long-duct nacelle also offers substantial drag reduction potential as a result of aerodynamic and propulsion improvements. The aerodynamic design and forthcoming test of the nacelle and pylon installation are described.

INTRODUCTION

The NASA Aircraft Energy Efficiency (ACEE) program has provided a stimulus to industry to accelerate development of technology directed toward energy savings and economic benefits. Under the ACEE Energy Efficient Transport (EET) program, Douglas is pursuing technology developments for potential application to the near-term derivatives of the DC-10 transport. The DC-10 is in extensive and successful use both in the United States and around the world in several versions. By the usual processes of product improvement, development is continuing in a number of areas. These developments are aimed at improvements in product durability, performance, and cost control. The value of the EET program is in the sponsorship of more advanced developments.

Of the advanced improvements possible, the aerodynamic development of winglets and of the long-duct nacelle (LDN) was selected for near-term work.

The function of the winglet is to reduce induced drag. The pictorial concept in figure 1 shows the DC-10 with winglets. The winglet is based on the classical design by Dr. R. T. Whitcomb of NASA Langley (reference 1), and, with his cooperation, has been the subject of considerable study at Douglas. In this form, the winglet consists of a near-vertical upper surface at each wing tip with a smaller lower surface ahead of it. The claimed advantage of a winglet over a wing-tip extension having the same drag reduction is a significantly smaller penalty on wing bending loads and hence a smaller weight penalty.

The purpose of the program is to develop the winglet to a high-potential drag reduction and compare it with wing-tip extensions.

*Including work performed under NASA Contract NAS1-14743

The LDN concept offers significant advantage in cruise efficiency through improvements in propulsive efficiency and the aerodynamics of the installation (reference 2). The work of reference 2 also explored the application of lightweight composite materials and the potential reduction in community noise. The representation in figure 2 shows a DC-10 equipped with the LDN. The LDN carries the outer (fan) duct past to the core nozzle, which incorporates a forced mixer. The advantages offered by this concept include the reduction of scrubbing and interference drag and an improvement in specific fuel consumption due to internal flow mixing.

The EET program concerns itself with the task of integrating the nacelle, pylon, and wing at high speed to achieve an installation with low interference drag.

SYMBOLS AND NOMENCLATURE

Values are given in SI Units and where appropriate also in U.S. Customary Units. Measurements and calculations were made in U.S. Customary Units.

A_c	Channel area, m^2
c	Local chord of wing, used in nondimensional parameter
c_ℓ	Section lift coefficient of local chord
c_R	Root chord of wing at aircraft centerline, used in nondimensional parameter
cc_ℓ/c_R	Nondimensional loading parameter
C_D	Drag coefficient
C_L	Lift coefficient
$C_{L_{W+B}}$	Lift coefficient, wing plus body
C_P	Pressure coefficient
L/D	Lift-to-drag ratio
M	Mach number
Range Factor	Lift-to-drag ratio multiplied by aircraft speed divided by fuel quantity used per unit propulsive thrust
W/δ	Aircraft weight divided by ratio of atmospheric pressure to atmospheric pressure at sea level on a standard day, kg (lb)
x/c_W	Distance from wing leading edge divided by wing chord

Subscripts not identified on previous page

L	Local
o	Freestream

WINGLET

A significant amount of design and analysis has already been performed on winglets for the DC-10. The current program introduces experimental methods to evaluate the aerodynamic potential. The process has the classical elements of design, test, and evaluation. The tests were completed on a 4.7-percent semispan DC-10 model in November 1977 in the NASA Langley 8-foot transonic wind tunnel.

Winglet Design

The basic DC-10 winglet is a Whitcomb design following general design guidelines published in reference 1. Prior to selection of test configurations, analytical studies were made using the Douglas Nonplanar Lifting Surface program (reference 3). Perturbations were made in height, taper ratio, location, upper surface/lower surface combinations, and size.

The analyses from these perturbations substantiated the Whitcomb design. The designs generally utilize a modified NASA GAW airfoil (reference,1), 65 percent wing-tip root chord, one tip chord height and with the winglet trailing edge coincident with the wing trailing edge. A typical design geometry is shown in figure 3. The use of the analysis of reference 3 suggests that there is an increase in winglet performance with forward movement of the upper winglet on the wing-tip chord. The risk in this approach is of interference drag due to the effect of the addition of the peak velocities of the wing and winglet.

Test Configuration

The aircraft configurations were chosen to identify the effect of winglets and of a wing-tip extension. The current DC-10 aircraft versions have been used as a basis, figure 4. The intermediate range DC-10 Series 10, with and without winglets, enables the effect of winglets to be established. This aircraft has a wing span of 47.35 meters (155 feet 4 inches). With the addition of the 3.08-meter (10-foot) span extension that converts the geometry of the Series 10 to that of the long-range Series 30/40, the effect of wing-tip extensions can be determined. With the addition of winglets to the Series 30/40, their effect can be measured and compared to those on the original Series 10.

The winglet configuration alternatives are shown in figure 5. For the Series 10, two chordwise positions were provided. Three winglet incidence angles were provided in each location. The lower winglet was made removable in order to measure effectiveness of the upper winglet with and without the lower winglet. For the Series 30/40, two winglets of different chords were provided to use the best winglet incidence angle from the Series 10 tests. The first winglet chord had the same chordwise proportions as the Series 10 winglet on the Series 10 wing. The second configuration was the Series 10 winglet, which resulted in larger winglet root chord relative to the wing tip chord. The root chord proportion in this case was 0.77.

Experimental Development

Force, moment and pressure data, as well as sufficient flow visualization data to assist in winglet configuration development, were obtained during the initial test. A loss of winglet effectiveness was observed as the Mach number approached cruise values. The reason for this was determined with the aid of oil flow visualization, figure 6. With only the upper winglet installed, the oil flow indicated a flow separation in the winglet root. With the lower winglet also installed, the flow separation transferred itself to the lower surface. The solutions to this difficulty were developed at the tunnel, and comprised wing-winglet juncture tailoring as well as physically moving the lower surface winglet forward to reduce upper and lower winglet interference. In the final winglet configurations little wing-winglet interference is believed present.

Winglet effectiveness is a strong function of the wing span loading without the winglet. A satisfactory correlation of wind tunnel test and flight loadings should indicate that the tunnel test properly simulates the environment for testing winglets and wing-tip extensions for the DC-10 models. Good correlation with flight test, and also with an earlier tunnel test of the DC-10-10 wing, was obtained as shown in the example in figure 7. The basic wing span loading used in the induced drag analysis was also consistent with that of wind tunnel and flight.

The winglet performance predicted from theory does not include viscous effects. It has been found (for example, reference 1) that the largest measured reductions of drag due to adding the winglet are obtained with normal loads on the winglet that are less than suggested as optimum by the theory. Viscous effects reduce the winglet loading potential relative to the analytical inviscid methods. Also, as loading on the winglet increases, viscous drag effects increase and apparently offset improvements in wing-winglet induced drag. It was therefore expected that the wind tunnel development would show the best performance with a winglet offloaded, that is having negative incidence as shown in figure 3. The test data indicated little sensitivity of drag reduction to winglet loading over an incidence range from 0^{o} to -4^{o}. However, a setting of -2^{o} appeared to be the best.

Tests were included to measure the effect of moving the winglet to the forward position on the Series 10 wing shown in figure 5. Oil flow visualization indicated no separation; however, results were inferior to the aft position. The Series 30 winglets previously described were also tested. The larger winglet tested showed a higher level of drag reduction.

Results and Comment

A summary of the principal results at specific cruise lift coefficients of the DC-10 Series 10 and Series 30/40 is shown in table 1. This identifies the reduction in drag coefficient obtained with the winglets installed relative to the wing without the winglets installed. It can be seen that the winglet gain is significant for both models. The Series 30/40 winglet has a slightly smaller gain. This difference is understood, and is due to the relatively washed-out tip extension utilized on the Series 30/40 wing.

Wind tunnel measured performance increments are shown in figure 8. Also shown are two levels of winglet performance estimates using the methods of reference 3. The optimum level of estimated performance occurred at 0 degree upper winglet incidence angle. However, the best test winglet incidence angle was off-loaded by 2 degrees (-2 degrees incidence angle). A second estimate line for the best winglet test configuration is also shown. As shown in the figure, the best winglets for both the Series 10 and Series 30/40 achieved drag reductions somewhat less than the full analytical potential.

However, for the case of reduced winglet incidence, the winglet data agree relatively well with analytical estimates. The measured performance improvement for the wing-tip extension (Series 10 to Series 30/40) also agrees well with the analytical estimate.

A fundamental winglet versus wing-tip extension comparison is shown in figure 9. Measured drag improvements and measured increases in wing-root bending moment for a fixed-lift coefficient of 0.5 are presented. The increase in wing-root bending moment due to a wing-tip device is indicative of the basic wing structural weight penalty for the inclusion of winglets or wing-tip extensions. As indicated, for a fixed value of drag improvement, winglets produce about one-half of the increase in wing-root bending moment as wing-tip extensions. Also, for the same increase in wing-root bending moment, winglets provide approximately twice the drag improvements as wing-tip extensions.

While the results of the high-speed testing are considered a success, the design of the wing and winglet at low speed and high lift requires further work. Furthermore, the characteristics of the entire aircraft with winglet installed remain to be determined.

LONG-DUCT NACELLE

The potential performance improvement offered by the long-duct nacelle on the DC-10 is significant. As a result of the combined improvements in external aerodynamics and internal flow mixing, the potential reduction in fuel burned is 4.5 percent for a typical long range mission. However, it is recognized that this nacelle installation requires at least as careful an aerodynamic design process as that for the current production short duct to avoid erosion of the potential gains. The principal considerations relate to the differences in the configurations, figure 10. The key area of interest to be discussed in this paper is the avoidance of any potential interference drag between nacelle, pylon, and wing due to the lengthening of the fan duct. This lengthening provides the opportunity for mixing of the fan and core flows. In addition, the fan flow is contained within the duct until aft of the core nozzle, reducing scrubbing losses on the core coil and pylon.

The objective of the program is therefore to develop a practical installation for the long-duct nacelle on the DC-10 which maximizes the potential reduction in fuel burned. The nacelle and pylon geometry has been developed analytically, with the evaluation to be based on experimental data. The test will be conducted in May in the Ames 11-foot facility, with a 4.7-percent DC-10 semispan model.

Basis for Design

Allowable configurations are those that retain the current DC-10 pylon primary structure. This approach minimizes changes in nacelle weight and center of gravity, with obvious and direct practical advantages in minimizing development costs and weight growth. Therefore, pylon shape development, to achieve an acceptable cruise configuration, is the primary area of effort.

However, in order to provide a spectrum of data, and as insurance should further improvements in interference drag be justified, a more forward position also will be tested.

High-speed interference drag in nacelle installation results from the effects of excessive velocity additions in the inboard channel formed by the wing nacelle and pylon. Examples of this difficulty are by the Convair 990 (reference 4) and the Douglas DC-8 prototype with long duct nacelle (reference 5).

These past experiences showed an unacceptable drag rise in the original configurations of the nacelle and pylon configurations. The relative shaping and disposition of these components relative to the wing resulted in additions of the flow velocities to an extent that shock wave losses and separation occurred. References 4 and 5 give explanations of the utilization of the area rule principle in solving these problems. The DC-8 prototype experience is summarized in figure 11. The original nacelle and pylon, while achieving the predicted improvements over the preceding short-duct nacelle at moderate Mach numbers, lost performance sharply at the higher Mach numbers desired for cruise. The reasons are reflected in the chart of nacelle pressure coefficients (figure 11), which indicates the strong shock condition. To achieve the desired gain throughout, the nacelle afterbody lines were refined (necessitating redesign of the thrust reverser), and an extended fairing was added to the pylon. This solution was satisfactory and complied with the intention to retain the basic pylon structure that existed.

The procedure described in reference 4 introduces a flow channel analogy by which designs may be evaluated for their interference effects. The flow channel is conventionally bounded by the wing, pylon and nacelle above the horizontal plane of symmetry, and by a suitable plane inboard of the pylon. In the Douglas work for the DC-10, an alternate approach for predicting pressures on the wing and nacelle has been adopted. This approach utilizes the Douglas Three-Dimensional Lifting Neumann program (DTLN). Figure 12 represents data from the two methods for the current DC-10 nacelle. As might be expected, the characteristics of the channel area distribution are consistent with the calculated wing lower surface pressure distribution.

Correlations of DTLN estimates of surface pressures with flight test data indicate that the modeling produces valid predictions in the vicinity of the pylon. A further simplification resulted from comparisons of wing-body-nacelle and wing-nacelle flowfield solutions. These showed little effect of the fuselage on the pressure distributions in the vicinity of the nacelle; therefore, in later analyses the body was eliminated to permit more detailed paneling of the nacelle and pylon.

The baseline LDN configuration employs the existing DC-10 pylon. This would result in the least cost solution if it could be shown not to incur an interference drag. Figure 13 illustrates a comparison of the calculated pressure distributions and channel area distribution for the DC-10 production short-duct and baseline LDN configurations. Both the suction peak under the wing and the subsequent adverse pressure gradient for the baseline are more severe than for the production DC-10. The calculated pressures for the baseline LDN are barely subcritical. The limitations of the Neumann potential flow (with compressibility corrections) method suggest that the baseline LDN configuration could exhibit excess nacelle interference drag.

Even though the wind-tunnel evaluation may show the baseline LDN to be acceptable, a contoured fairing to the pylon does tend to reduce the local Mach number in the channel. Contoured designs have been designed with the aid of the DTLN.

Among the designs considered is that illustrated in figure 14. The contour is applied to the aft fairing of the pylon, thus retaining intact the primary structure. This contour tailors the pressure distributions in the potentially critical regions. Figure 14 shows that the contouring significantly improves the suction areas and adverse pressure gradients on both the wing lower surface and the nacelle afterbody. Figure 13 and 14 wing lower surface pressure coefficients are generally comparable although detailed variations exist due to the use of slightly different panelling distributions. By such contouring, the possibility exists of achieving interference drag as low as or even better than the current production nacelle.

Experimental Program

The test configurations consist of an unpowered flowthrough and a powered current production nacelle and pylon, a number of pylon configurations with an unpowered flowthrough LDN, and an LDN with a powered engine simulator. The power plant represented in the nacelle design is the General Electric CF6-50 Series used on the DC-10 Series 30. It is considered that the results will be representative of the Pratt and Whitney engines used on the DC-10 Series 40.

Overall configuration forces and moments, nacelle normal force, and wing/nacelle/pylon (inboard side only) pressure data will be recorded. Test configurations will be evaluated at cruise Mach number over the range of lift coefficient applicable for cruise conditions. This will require Mach numbers of 0.8 to 0.84 and angles of attack from 1.5 to 3.5 degrees. The relative effect of simulated engine power on the interference drag of the baseline configuration will be recorded. The test will cover fan pressure ratios of 1.0 to approximately 1.6. Flow visualization will be employed, using fluorescent minitufts.

This phase of the long-duct nacelle programs focuses on high-speed development which must be the foundation for a production design. Further development on the installation and determination of characteristics for the aircraft at both high and low speeds will be necessary.

CONCLUDING REMARKS

Douglas, under the Aircraft Energy Efficiency (ACEE)/Energy Efficient Transport (EET) program, is pursuing advanced technology developments toward fuel savings on near-term DC-10 derivatives. Specific major thrusts are development and wind tunnel evaluation of winglets on the DC-10 Series 10 and Series 30/40 configurations and definition of Long-Duct Nacelle (LDN) configurations that will not be severely penalized by interference drag.

For equivalent drag reduction, winglets yield about one half of the increase in wing root bending moment as wing-tip extensions.

Analysis indicates the possibility of LDN and pylon configurations having an interference drag equal to or better than the current CF6-50C configuration. Wind tunnel tests to confirm this are planned.

REFERENCES

1. Whitcomb, Richard T.: A Design Approach and Selected Wind Tunnel Results at High Subsonic Speeds for Wing-Tip Mounted Winglets. NASA TN D-8260, July 1976.

2. Nordstrom, K. E.; March, A. H.; and Sargisson, D. F.: Conceptual Design Study of Advanced Acoustic Composite Nacelles. NASA CR 132703, July 1975.

3. Goldhammer, M. I.: A Lifting Surface Theory for the Analysis of Nonplanar Lifting Systems. AIAA Paper No. 76-16, January 1976.

4. Kutney, John T.; and Piszkin, Stanley P.: Reduction of Drag Rise on the Convair 990 Airplane. J. Aircraft, Volume 1, No. 1, January 1964.

5. Lynch, F. P.: Summary of Results from DC-8 Ship 201 Long-Duct Pod Flight Development Program. Douglas Aircraft Company, Report No. LB 32668, September 1965.

TABLE 1
WINGLET – MEASURED DRAG REDUCTIONS

REDUCTIONS IN DRAG COEFFICIENT, SHOWN FOR TYPICAL CRUISE LIFT COEFFICIENTS

M	BEST SERIES 10 WINGLET $C_L = 0.45$	SERIES 10 TO 30 TIP EXTENSION $C_L = 0.45$	BEST SERIES 30 WINGLET $C_L = 0.50$
0.82	0.0011	0.0009	0.0009
0.74	0.0010	0.0007	0.0010
0.60	0.0011	0.0007	0.0008

Figure 1.- DC-10 with winglets.

Figure 2.- DC-10 with long-duct nacelles.

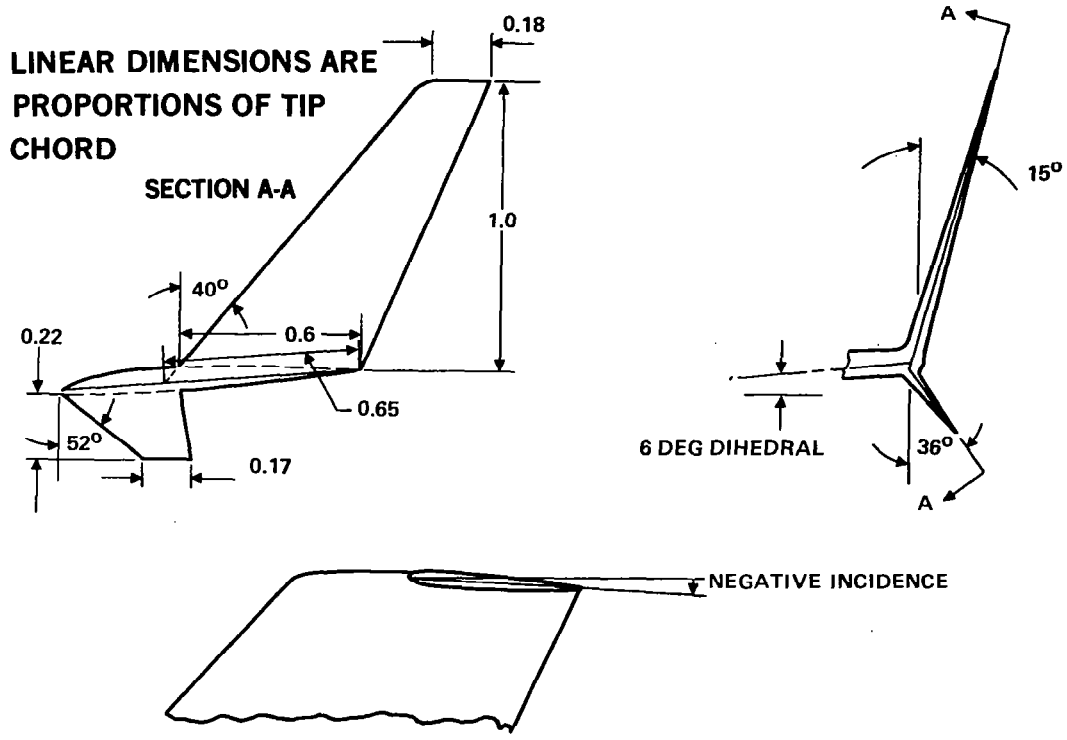

Figure 3.- Winglet - typical geometry.

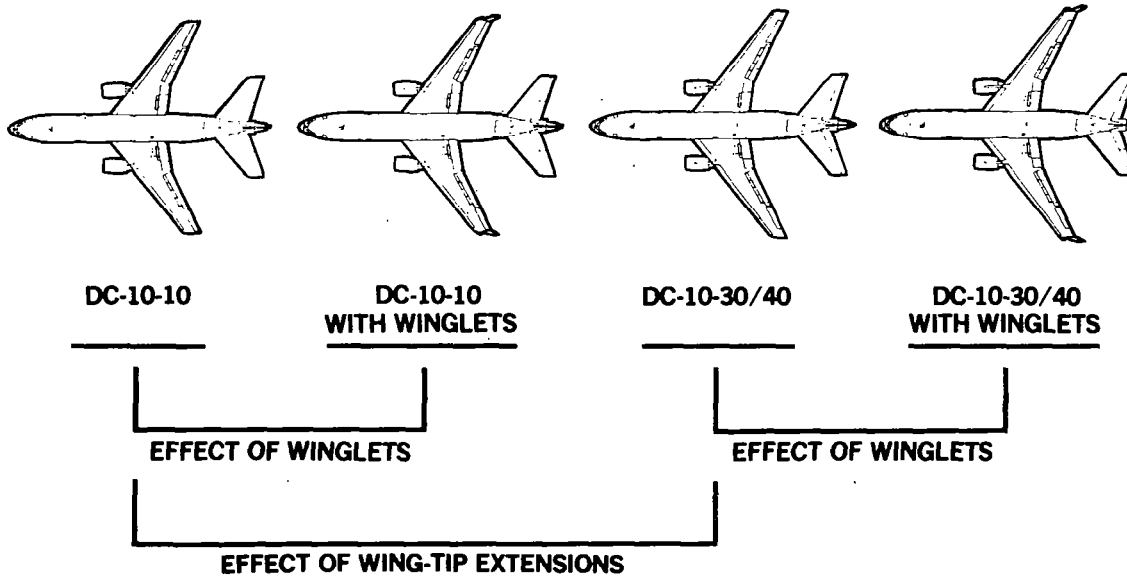

Figure 4.- DC-10 aircraft configurations for evaluation.

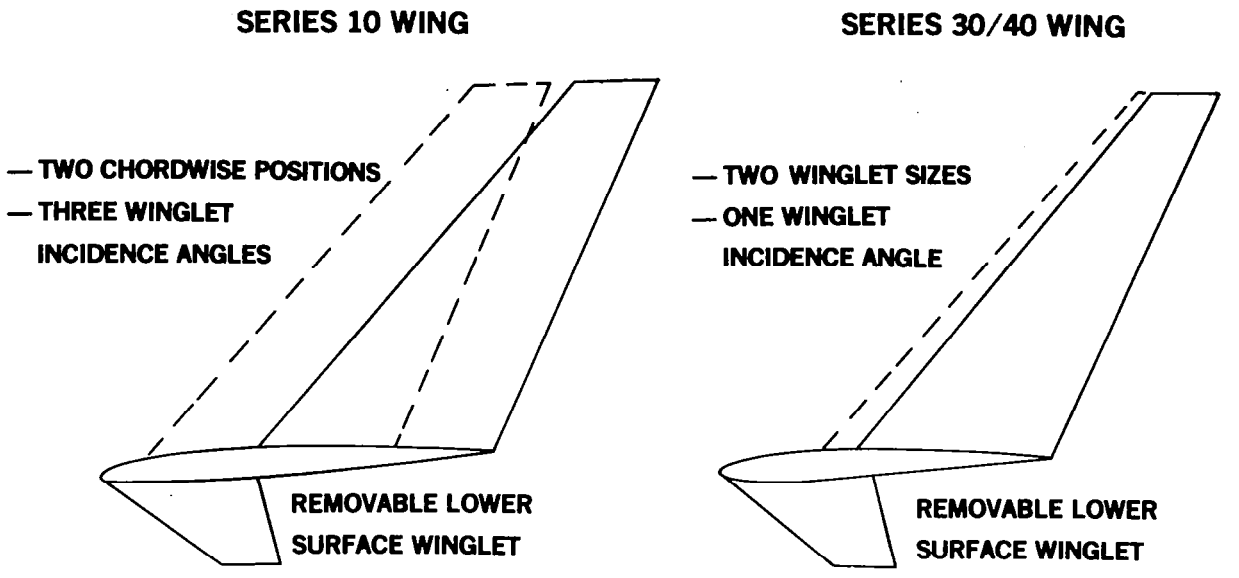

Figure 5.- Winglet test configurations.

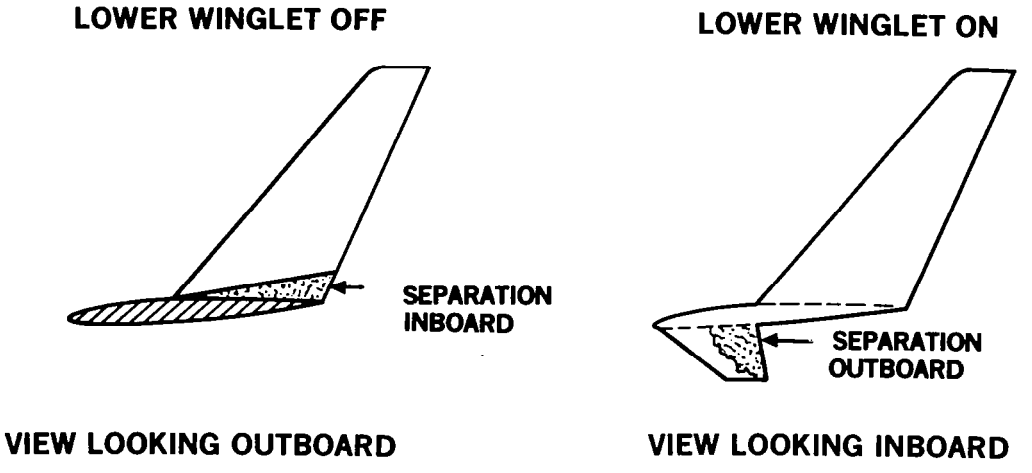

Figure 6.- Initial viscous problems.

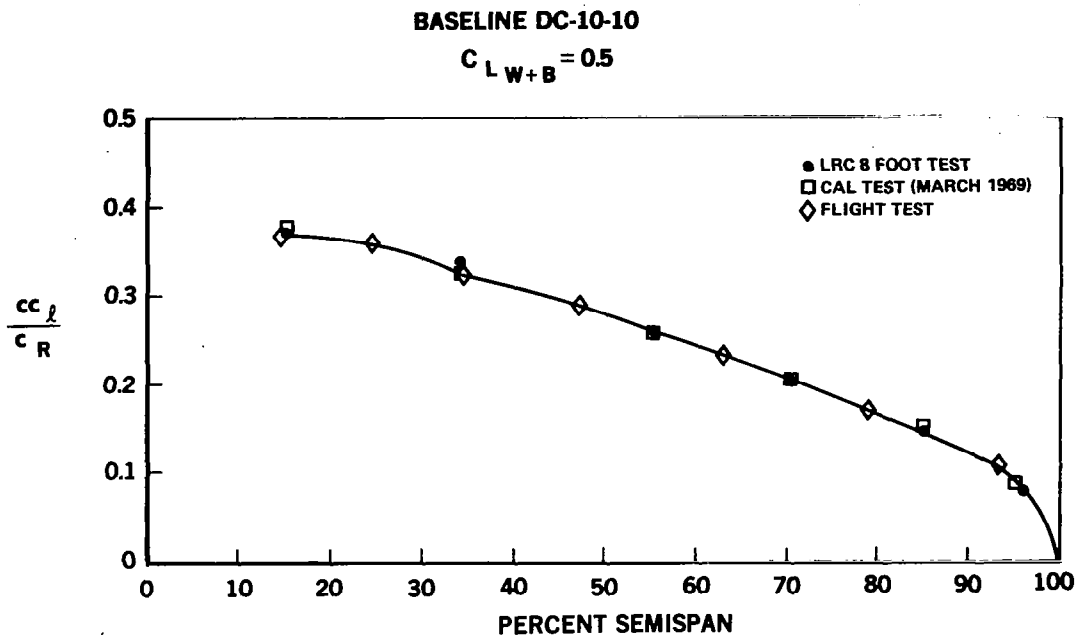

Figure 7.- Wing span loading comparison.

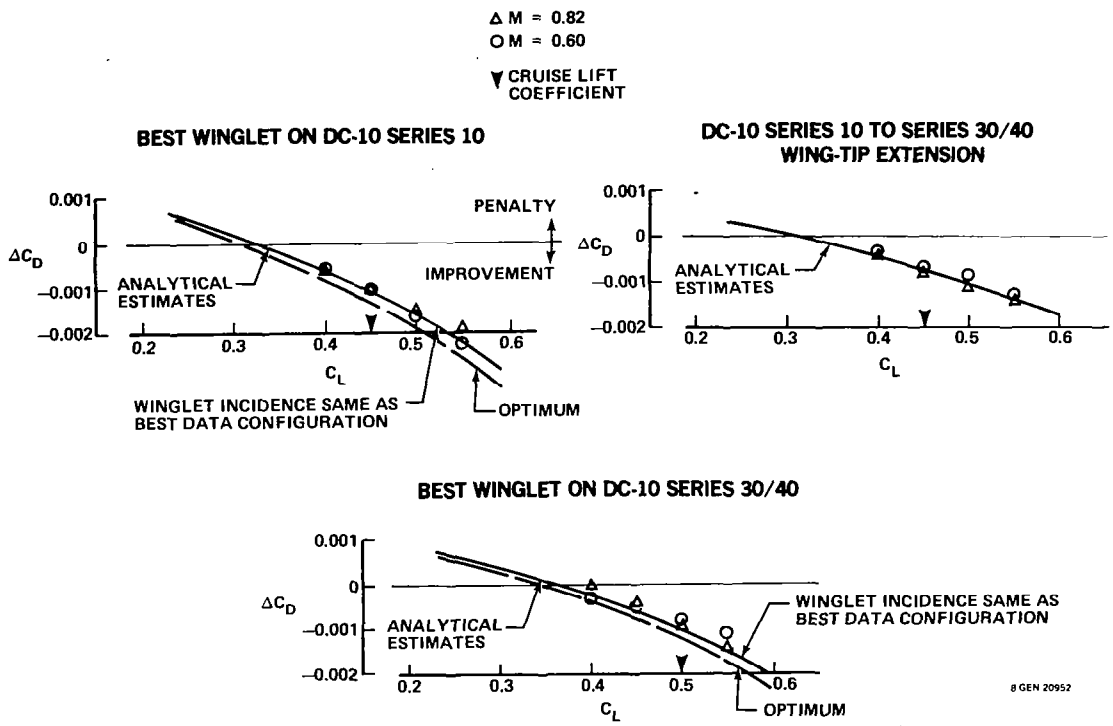

Figure 8.- Incremental cruise drag results.

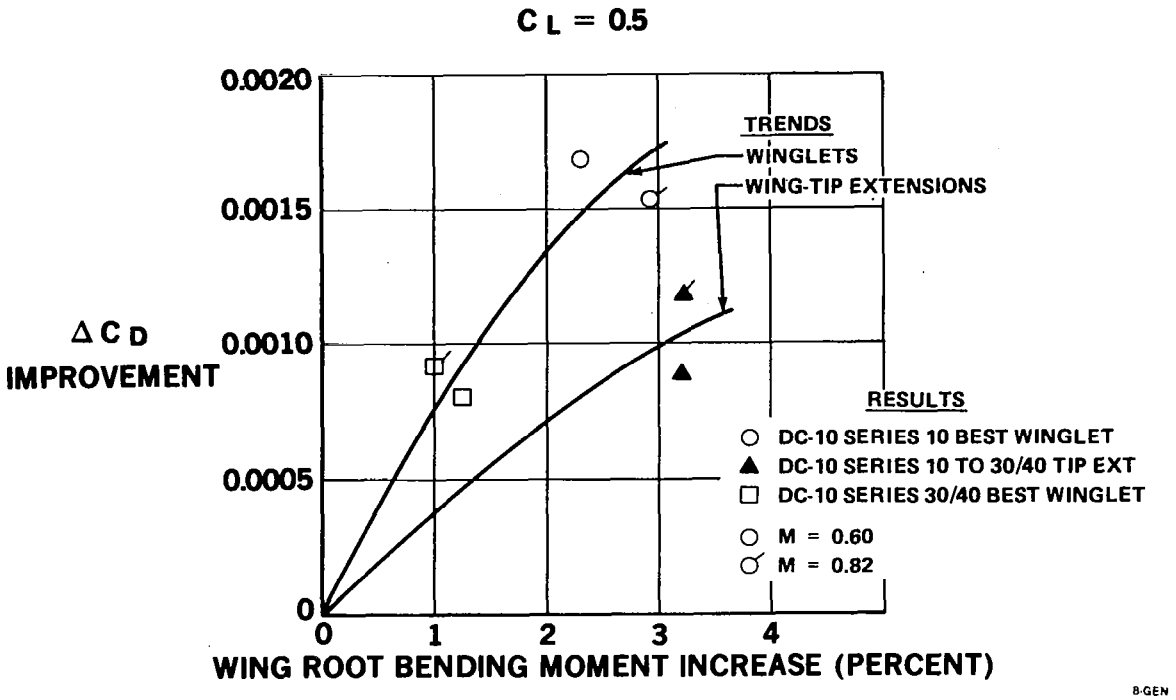

Figure 9.- Measured effects of winglets and a wing tip extension on drag and root bending moment.

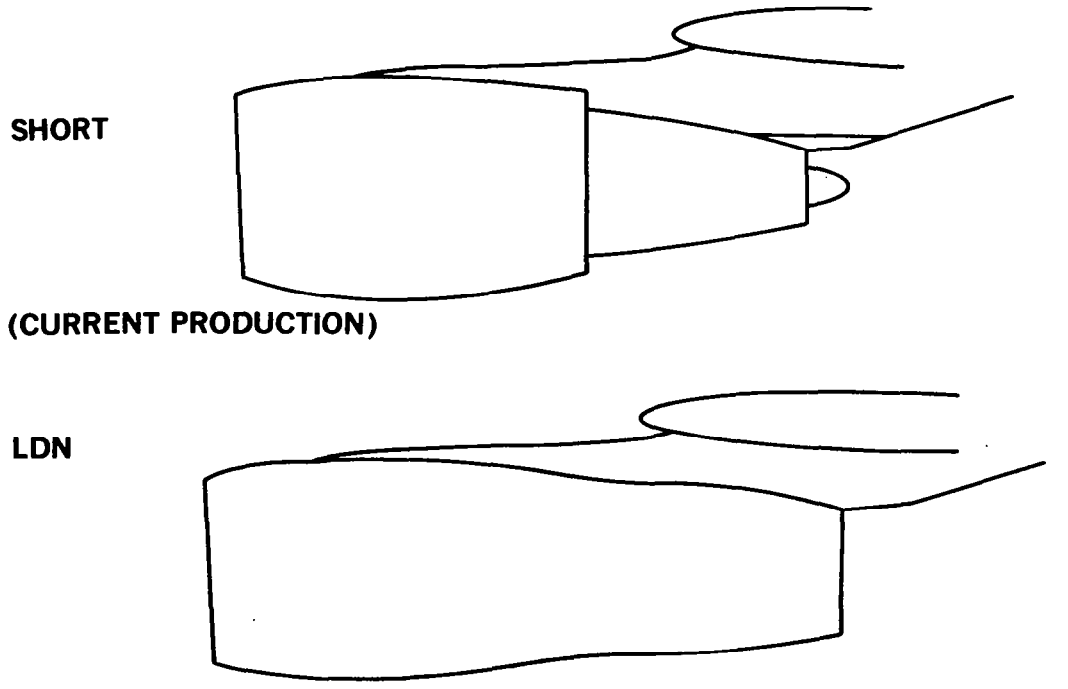

Figure 10.- Comparison of short- and long-duct nacelle shapes.

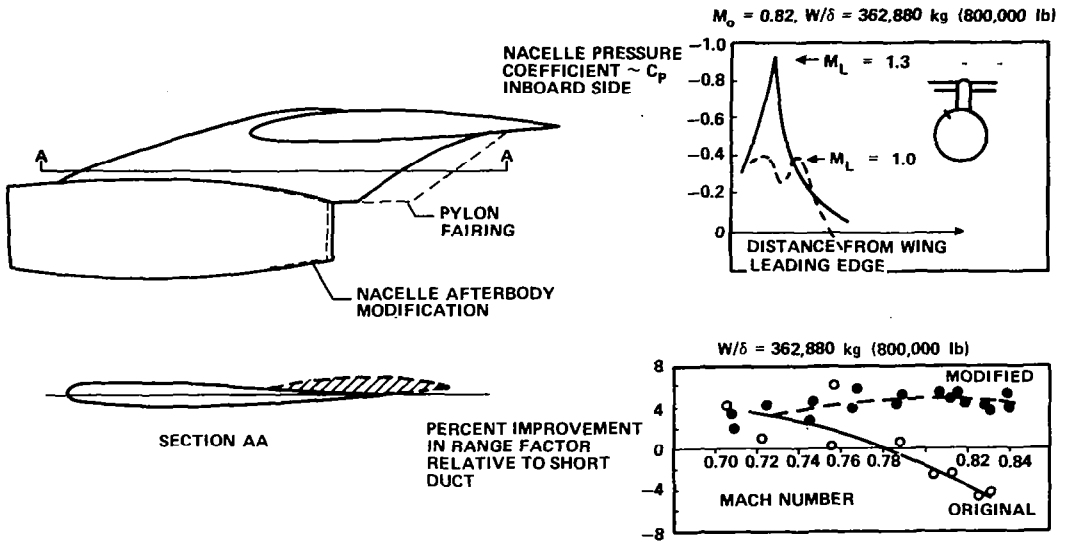

Figure 11.- Prototype DC-8 - effect of nacelle/pylon/wing interference drag.

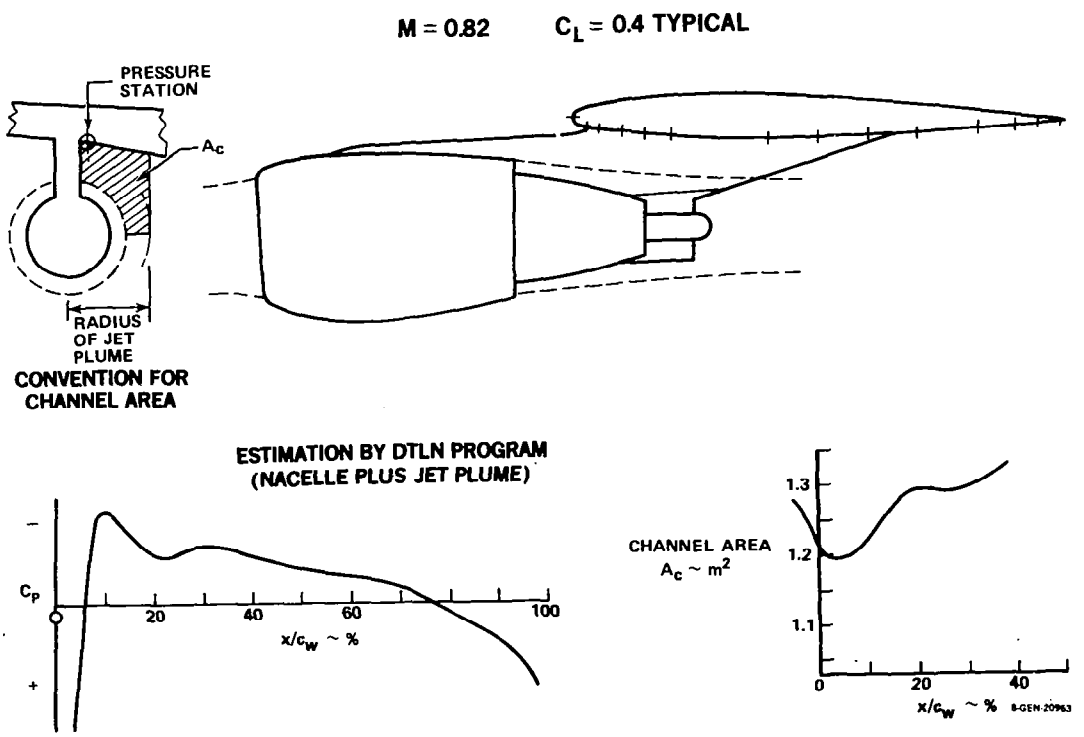

Figure 12.- Flow representations for production nacelle.

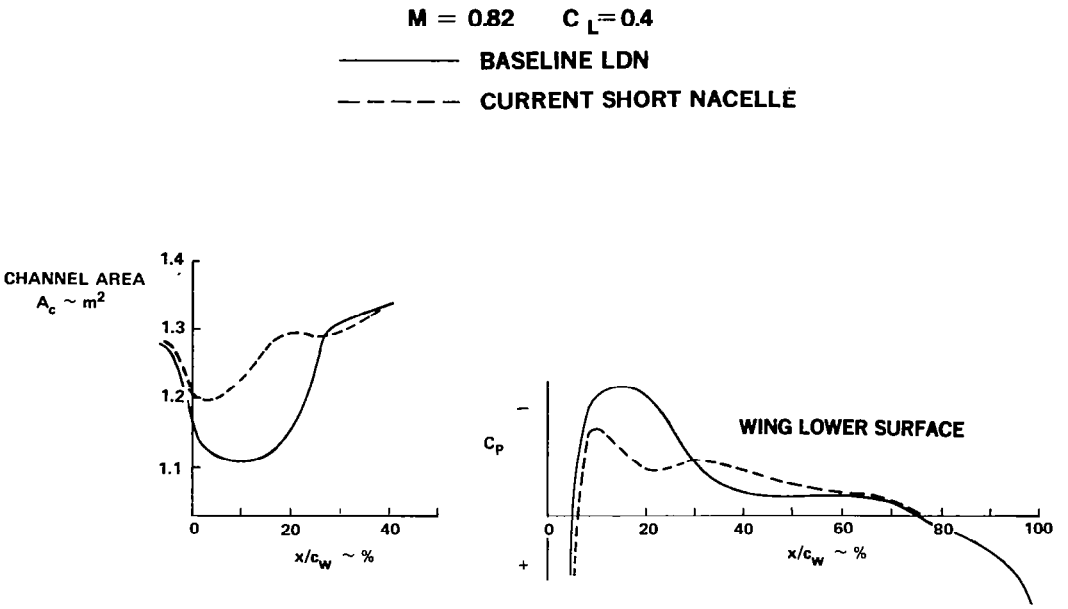

Figure 13.- Flow representations - LDN baseline.

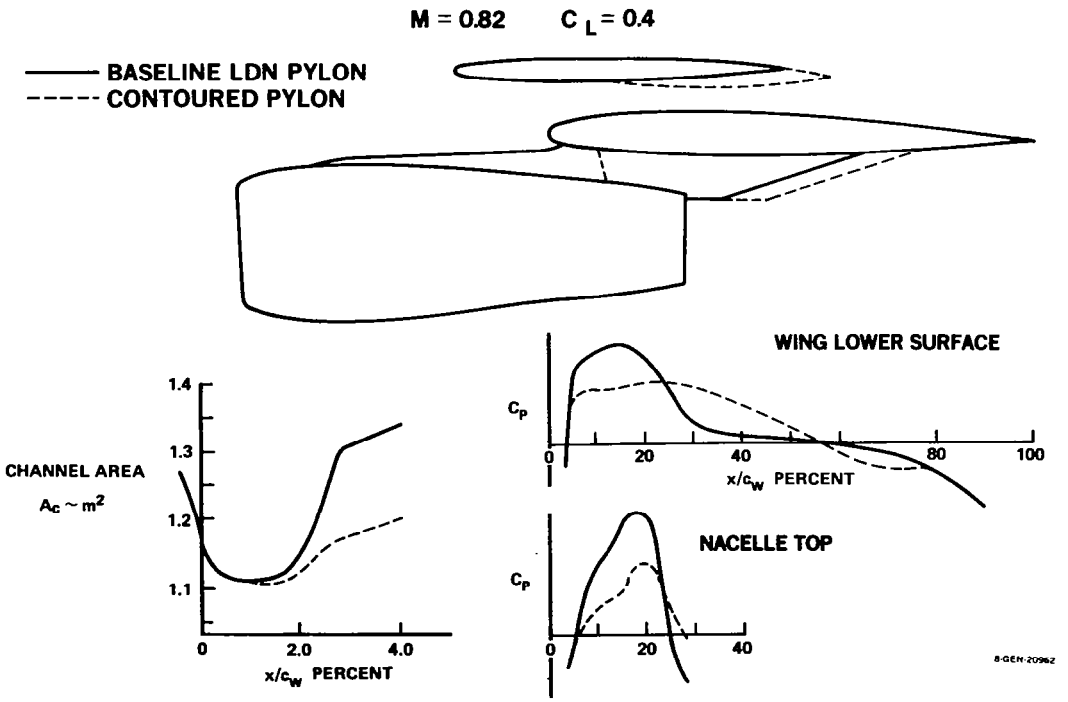

Figure 14.- Flow representations - improved pylon.